Eur Biophys J (2012) 41:209–215
DOI 10.1007/s00249-011-0777-1

ORIGINAL PAPER

EBSA
Biophysics in Europe

Comparative electrochemical study of superoxide reductases

Cristina M. Cordas · Patrícia Raleiras · Françoise Auchère · Isabel Moura · José J. G. Moura

Received: 19 August 2011 / Revised: 29 October 2011 / Accepted: 21 November 2011 / Published online: 6 December 2011

Abstract Superoxide reductases are involved in relevant biological electron transfer reactions related to protection against oxidative stress caused by reactive oxygen species. The electrochemical features of metalloproteins belonging to the three different classes of enzymes were studied by potentio-dynamic techniques (cyclic and square wave voltammetry): desulfoferrodoxin from *Desulfovibrio vulgaris* Hildenborough, class I superoxide reductases and neelaredoxin from *Desulfovibrio gigas* and *Treponema pallidum*, namely class II and III superoxide reductases, respectively. In addition, a small protein, designated desulforedoxin from *D. gigas*, which has high homology with the *N*-terminal domain of class I superoxide reductases, was also investigated. A comparison of the redox potentials and redox behavior of all the proteins is presented, and the results show that SOR center II is thermodynamically more stable than similar centers in different proteins, which may be related to an intramolecular electron transfer function.

C. M. Cordas (✉) · P. Raleiras · F. Auchère · I. Moura · J. J. G. Moura
REQUIMTE, CQFB/FCT, Departamento de Química, Universidade Nova de Lisboa, 2859-516 Caparica, Portugal
e-mail: cristina.cordas@dq.fct.unl.pt

Present Address:
P. Raleiras
Department of Photochemistry and Molecular Science, P.O. Box 523, 75120 Uppsala, Sweden

Present Address:
F. Auchère
Laboratoire Mitochondries, Métaux et Stress Oxydatif, Institut Jacques Monod, UMR 7592
CNRS—Université Paris-Diderot, Paris, France

Keywords Electrochemistry · Metalloproteins · Iron–sulfur centers · Superoxide reductases

Introduction

The superoxide reductase (SORs) proteins are responsible for the one-electron reduction of O_2^- to H_2O_2 and have a role in protection against oxidative stress (Lombard et al. 2000). So far, three classes have been recognized, according to domain organization and metallic center complements. Members of class I contain two domains with two types of iron centers, respectively: $Fe(S–Cys)_4$ (center I) and $Fe(S–Cys)(N–His)_4$ (center II), the catalytic site. Iron in center I is coordinated to four cysteines in a tetrahedral arrangement, and in center II, the metal has a square pyramidal geometry with four equatorial histidines and an axial cysteine (Pereira et al. 2007). Class II proteins are shorter and contain only one domain with center II. Class III also has only one metallic center, like class II proteins, but presents another domain, similar to class I but with no metallic center (Moura et al. 1990; Niviere and Fontecave 2004). In Table 1, a summary of the three classes is presented.

Desulfoferrodoxin (Dfx) is classified as a class I SOR and is a homodimeric protein, with 14 kDa. Neelaredoxin (Nlr), isolated from *Desulfovibrio gigas* (*Dg*) and *Treponema pallidum* (*Tp*), belongs to class II and III SORs, respectively, and has ca. 15 kDa (Ascenso et al. 2000; Rusnak et al. 2002). This protein has an iron center coordinated by four equatorial histidines, which in Nlr from *Tp* are His16, His41, His47 and His114, and an axial cysteine, Cys111, in the reduced state. In the oxidized state it can also present an extra axial ligand, Glu14. This structural difference between redox states has been related to the

Table 1 Summary of the proteins used in this study

Proteins	Class	Organism	Center I	Center II	MW/kDa
Dfx	I	*Dv*	$Fe(S–Cys)_4$	$Fe(S–Cys)(N–His)_4$	14
Nlr	II	*Dg*	–	$Fe(S–Cys)(N–His)_4$	15
Nlr	III	*Tp*	–	$Fe(S–Cys)(N–His)_4$	15
Dx	(Not SOR)	*Dg*	$Fe(S–Cys)_4$	–	4

catalytic activity of the enzyme regulating the access of the superoxide anion to the center (Rusnak et al. 2002; Yeh et al. 2000). This Nlr center has high homology with class I SOR proteins (center II).

Desulforedoxin (Dx) is a small homodimer protein (about 4 kDa) with high homology with class I SOR domain I, as the iron coordination in both proteins is assured by four cysteines with similar geometry (Coelho 1997; Archer et al. 1995). They differ from regular rubredoxins as two of the cysteinyl ligands are placed adjacently.

Dfx was found in different strains such as *Desulfovibrio desulfuricans* (*Dd*) ATCC27774 and *Desulfovibrio vulgaris* (*Dv*) Hildenborough, but not in *Dg*, while Dx (analogous to SORs center I) and Nlr (devoid of center I) were found in the latter, but not in the former two. This fact makes Dx a putative candidate for a redox partner of Nlr (Auchère et al. 2006), suggesting that different methods may be used to achieve electron transfer to center II, using intrinsic build-up center I or the interaction with a carrier that contains an analogue of center I (Dx). The comparison between the structural features of these proteins and their operating redox potentials is a step toward understanding the role of the two iron centers in the SOR proteins.

Direct electrochemistry of redox proteins is an important and attractive subject because it provides a tool to determine redox potentials and to study the mechanisms of electron exchange in relevant biological systems as well as protein-partner recognition (Hagen 1989; Hu 2001). Different approaches to achieve this unmediated response are, for instance, the use of modified electrodes with specific films that can incorporate or interact with the target proteins, such as polycations (Lu et al. 2000), surfactants (Chattopadhyay 2000; Bianco 1997), polymers (Hu 2001; Os et al. 1996) and several self-assembled monolayers (Li 1997; Allen et al. 1984), among others. Also, the electrode modification with protein films led to a technique called Protein Film Voltammetry, with good results (Hirst 1998; Angove et al. 2002). The physical immobilization of proteins on the electrode surface by the use of membranes is another possible procedure that has been used with success in past years. In this work, this latter approach was chosen, taking into consideration the systems under study versus the advantages of the technique, relative to modified electrodes and "classic" bulk solution electrochemistry (Lojou 2000; Correia dos Santos et al. 2003). The use of small volumes of protein, the easy preparation and low cost of the electrodes, and the approximation to thin layer theory are positive points to take into consideration (Brett and Brett 1996; Laviron 1979). Some modifiers were used, namely neomycin sulfate for glassy carbon (GC) and 4,4′-dithiodipyridine for gold, aiming to improve the interaction between the proteins and the electrode surfaces, as has been currently reported by several authors (Allen et al. 1984; Correia dos Santos et al. 2001, 2003; Isao Taniguchi et al. 1986). The carbon surface (due to the carboxylic, phenolic and quinonoidal groups) (Razumas et al. 1984) and the dialysis membrane (cellulose), at experimental conditions, as well as the enzyme surfaces were negatively charged, so magnesium cations were added to the electrolyte solution. The inclusion of the Mg^{2+} should assure charge compensation and may promote better interaction between the electrode and the proteins (Fraser et al. 1987), allowing obtaining an enhanced current response.

The electrochemical responses of the Dx from *Dg* to different classes of SOR proteins (Dfx from *Dv* to Nlr from *Dg* to *Tp*) were evaluated by cyclic and square wave voltammetry on both GC and gold electrode materials. The proteins' electrochemical behavior was studied on different materials since there is a diversity of affinity of different proteins toward different electrode surfaces. To properly compare the proteins' features, it is important to ensure that differences found in the centers' redox potentials are not due to experimental artifacts such as surface affinity.

Materials and methods

The potentio-dynamic experiments were performed with an AUTOLAB PGSTAT 12 potentiostat/galvanostat. A three-electrode configuration in a one-compartment electrochemical cell was used. GC and gold with 0.06 and 0.12 cm^2, respectively, were the working electrodes. A platinum wire and saturated calomel (SCE) were the counter and reference electrodes. The GC electrode had been previously treated by immersion in concentrated nitric acid, rinsing with water, polishing with 1.0 and 0.3 μm alumina, sonication (10 min) and thoroughly rinsing with Millipore water. The gold electrode was treated the same way except for the nitric acid immersion. For the GC electrode, pre-conditioning in 2 mM neomycin sulfate

solution and 1 mM 4,4′-dithiodipyridine for gold was performed for 10 min. Protein immobilization was accomplished with a membrane [Medicell visking dialysis membrane (cellulose), 3,000 or 12,000–14,000 Da cutoff] adjusted to the electrodes with a rubber *o*-ring. The supporting electrolyte was 10 mM Tris-HCl buffer, pH 7.6/0.1 M KNO_3/2 mM neomycin sulfate and 20 mM $MgCl_2$. Cyclic voltammetry (CV) was performed at different scan rates (from 1 to 200 mV/s), and in the square wave voltammetry (SWV) 50 mV pulse amplitude, 1-mV step, and frequencies between 8 and 143 Hz were used. The proteins were purified as described elsewhere (Moura et al. 1990; Ascenso et al. 2000; Czaja et al. 1995; Auchère et al. 2004), and the concentration of the proteins samples was ca. 300 μM. All values were reported to the Normal Hydrogen Electrode (NHE), and values are indicated in mV.

Results and discussion

Desulforedoxin (Dg)

The electrochemical responses of *Dg*Dx on the different working electrode surfaces, namely GC and gold, were attained using the membrane system. Only one redox process was observed at different scan rates, corresponding to the oxidation/reduction of the metallic center $[Fe(S–Cys)_4]^{3+}/[Fe(S–Cys)_4]^{2+}$ (Fig. 1a), with sharper and more defined peaks being observed on the GC electrode. On gold (data not shown), the same process presents a broader shape of the observed anodic peak, which might be a consequence of possible interactions between the molecules at the electrode surface, which is a well-described phenomenon of surface-confined species (Laviron and Roulluier 1980).

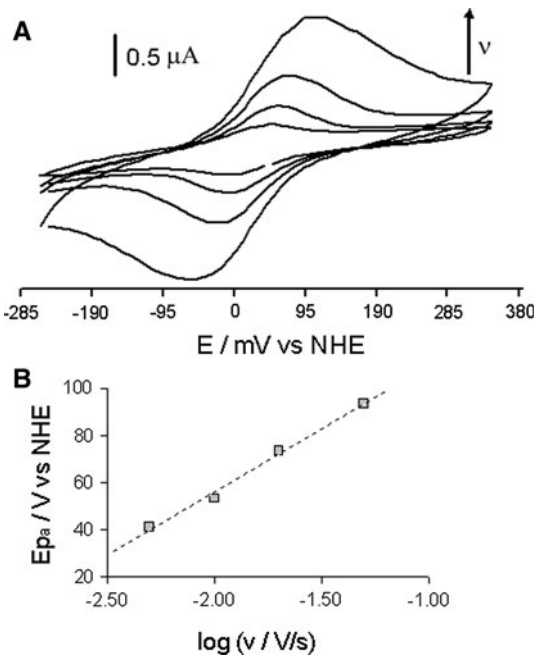

Fig. 1 **a** Dx cyclic voltammograms at different scan rates (1, 2.5, 5 and 8 mV/s) on GC; **b** *plot* of the Dx peak potentials, E_p, dependence on log *v*, obtained by CV on the GC electrode

Membrane-confined Dx has electrochemical behavior according to the Thin Layer Theory (Brett and Brett 1996; Laviron 1979). The current intensity varies linearly with the scan rate (up to 20 mV/s), and the difference between the potential values of the anodic and the cathodic peaks, ΔE, also depends on the scan rate; linearity is better for small scan rates. The mean value of the oxidation and the reduction peak current potentials remains constant within the imposed conditions. The slope of the plot E_{pa} versus log *v* is 53 mV/log unit (Fig. 1b), which is close to the expected theoretical value (Laviron 1979). Assuming an electrochemical transfer coefficient of 0.5 and using the theoretical curves of Laviron (1979), it was possible to estimate the apparent heterogeneous electron transfer coefficient, ks, values which were shown to be scan rate dependent, as already reported in the literature for different non-diffusion systems (Zhang and Rusling 1997). The maximum ks value calculated was 11.7 s^{-1} for a 50 mV/s scan rate.

The formal reduction potential, $E^{o\prime}$, was estimated by the $(E_{pa} + E_{pc})/2$ values, and the result found for the Dx redox process was similar with both electrode materials, namely $+24 \pm 8$ for GC and $+28 \pm 5$ mV versus NHE for gold. Also by SWV, a well-defined response of Dx on both electrodes was obtained (not shown). The obtained E_p is $+5 \pm 8$ and $+5 \pm 7$ mV versus NHE, respectively, on GC and gold electrodes. The difference with the CV data may be related to the technique used. In fact, some factors may lead to small differences on the obtained formal potentials using the two techniques, such as dispersion of the redox formal potentials or spatial distribution (Zhang and Rusling 1997). The protein presents reversible behavior in both materials with values for the peak width at half current height ($W_{1/2}$) of approximately 127 mV, which is close to the theoretical value of 124 mV at experimental conditions. Due to the small SWV diffusion layer thickness, when compared with the membrane layer thickness (around 12 μm), it is considered that the results should be analyzed considering diffusion control, as shown by some authors (Correia dos Santos et al. 2003). The heterogeneous charge rate constant, K_{sh}, of the redox process on GC was calculated based on Laviron's mathematical formulation (Laviron 1979), and the value, 2.43×10^{-4} cm s^{-1} (GC, CV), is in agreement with others published for small metalloproteins (Correia dos Santos et al. 2003). The addition of a multivalent cation, Mg^{2+}, to the electrolyte enhances the faradic response, as expected, since the

carbon protein surface, at pH 7, and the dialysis membrane used to perform the immobilization all have negative charges; this magnesium addition, however, is not crucial for obtaining reasonable signals for Dx.

Neelaredoxin (Nlr)

The electrochemical behavior of two Nlrs from *Dg* (class II SOR) and from *Tp* (class III SOR) was assessed by cyclic and SWV techniques.

Nlr from Dg, class II SOR

The electrochemical behavior of the *Dg*Nlr was tested both in GC and gold electrodes, showing roughly defined cyclic voltammograms. The electroactivity lowers significantly with the number of potential scans. A reduction peak at −169 mV and poorly defined oxidation wave at −42 mV were observed (data not shown). Better results, however, were attained with the SWV technique, as observed in Fig. 2. It was possible to observe well-defined bell-shaped current/potential curves, and the E_p and $W_{1/2}$ values remained constant with the frequency increase. The calculated $E^{o\prime}$s were -92 ± 9 and -30 ± 10 mV, respectively, on GC and gold electrodes, scanning in the cathodic direction. The obtained forward, I_f, and backward, I_b (not shown), currents for this system are compatible with the typical profile for a reversible process. The value of $W_{1/2} \approx 86$ mV was, however, lower than expected for reversible electrochemical behavior. This may be related to adsorption phenomena on the electrode surface (Souza et al. 2003) and changes from a regime of unrestricted to restricted diffusion (Kounaves et al. 1987). The I_p presented good linearity with the increase of the frequency rather than with the square root of the frequency, denoting again a shift from what was expected for reversible behavior.

Nlr from Tp, class III SOR (center II)

The *Tp*Nlr presented a better electrochemical response by CV than the *Dg*Nlr, showing a negligible decrease in electroactivity after ten cycles. The current peaks due to the redox process $[Fe(S–Cys)(N–His)_4]^{3+}/[Fe(S–Cys)(N–His)_4]^{2+}$ on gold can be seen on Fig. 3. The current peaks increased linearly with the scan rate, and the $(E_{pa} + E_{pc})/2$ values were constant. The calculated formal potential was 11 mV. The SWV response for the *Tp* Nlr showed a shift of E_p toward more negative values and the enlargement of the peak width with the frequency increase (Fig. 4a), which might be related to lower reversibility associated with this redox process (Osteryoung and Rao 1885). For the 8 Hz frequency used, scanning in the cathodic direction, the E_p value was -97 ± 6 mV. The profile of the I_f and I_b currents, however, still seemed compatible with a reversible process (Fig. 4b).

Dfx from Dv, class I SOR (centers I and II)

The typical voltammetric behavior of Dfx on GC is displayed in Fig. 5. A cathodic wave at approximately −52 mV and the corresponding anodic process around 50 mV were observed at 1 mV/s. By comparison with the Dx results and previous results of a recombinant Dfx protein (DfxN), with only one metallic center (center I) (Ascenço 2001), these current peaks were indexed to the Dfx center I redox process, $[Fe(S–Cys)_4]^{3+}/[Fe(S–Cys)_4]^{2+}$. Although the observed results shifted from ideal electrochemical behavior, the $(E_{pa} + E_{pc})/2$ values were still constant, within experimental error, allowing us to estimate the formal potential ($E^{o\prime} = -14 \pm 11$ mV, CV, pH 7.6, room temperature). The same process at the gold electrode reveals similar features, but with enhanced irreproducibility and irreversible character (not shown). The SWV response (shown later in the text within the comparison with the other proteins) for the Dfx (center I) at GC and gold showed a linear dependence of the peak current

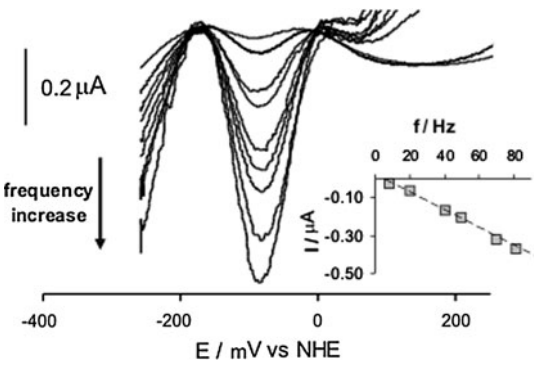

Fig. 2 *Square wave* voltammogram of the Nlr (*Dg*) on GC at different frequencies (8, 20, 40, 50, 70, 81, 96, 120, 143 Hz), 10 mV step potential and 50 mV amplitude

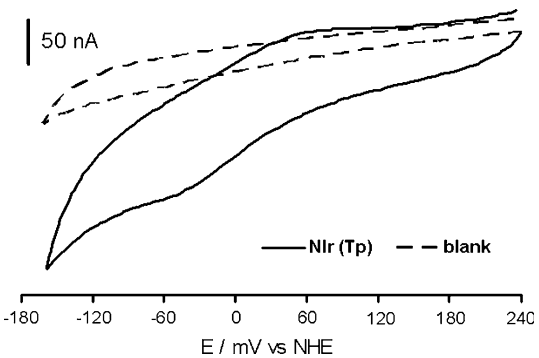

Fig. 3 Cyclic voltammograms of the Nlr (*Tp*) on gold and comparison with the blank, $v = 4$ mV/s

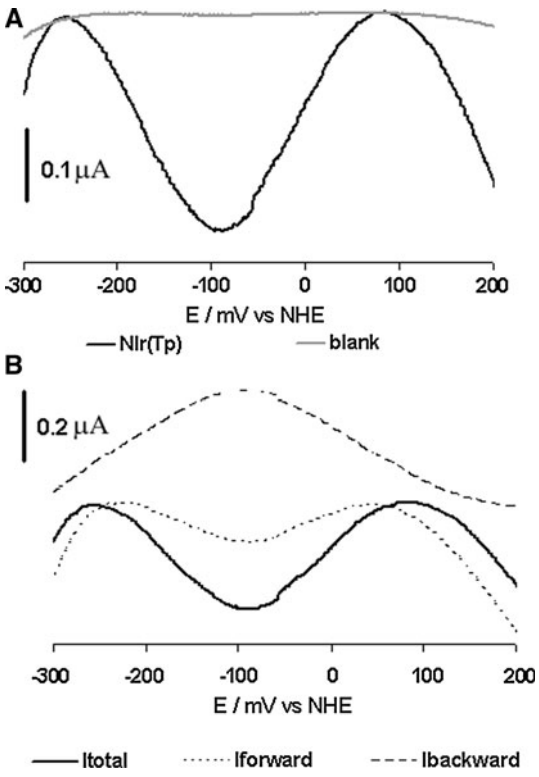

Fig. 4 *Square wave* voltammograms of the Nlr (*Tp*) on gold and comparison with the blank (**a**), and *plot* of the I_{total}, $I_{forward}$ and $I_{backward}$ for the same Nlr (*Tp*) essay (**b**); 10 mV step potential, 50 mV amplitude and frequency 8 Hz

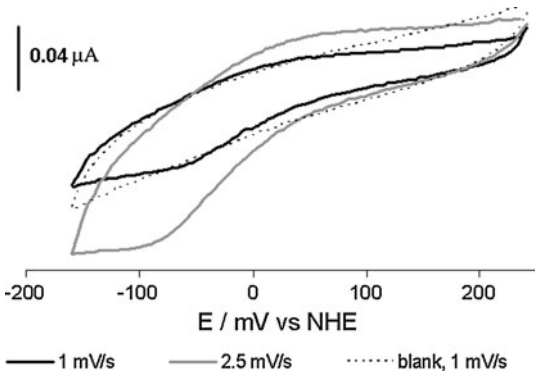

Fig. 5 Cyclic voltammograms of Dfx and comparison with the blank obtained on GC

intensity with the applied frequency (from 8 to 143 Hz). On the gold electrode the E_p and $W_{1/2}$ values remained constant, namely -10 ± 5 and $+92$ mV, and this last value ($W_{1/2} \approx 92$ mV) was also lower than expected for a completely reversible process (Fig. 6). Some preliminary studies by SWV, scanning in the anodic direction, allowed observation of another process around 400 mV (labeled with a question mark in the legend of Fig. 7). This process was not reproducible and was only observed at the first anodic scan of each assay. Previous results of recombinant

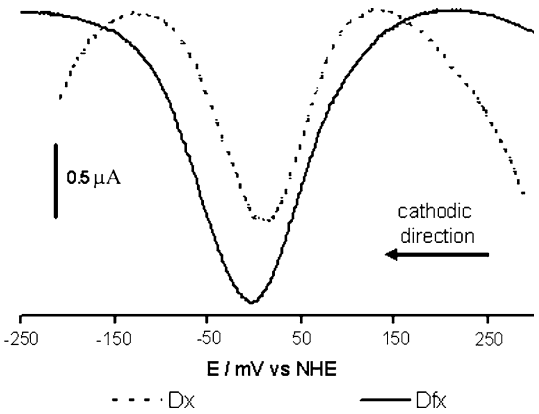

Fig. 6 Comparison between the square wave responses of the Dfx (center I) and Dx on gold; 10 mV step potential, 50 mV amplitude and 8 Hz frequency

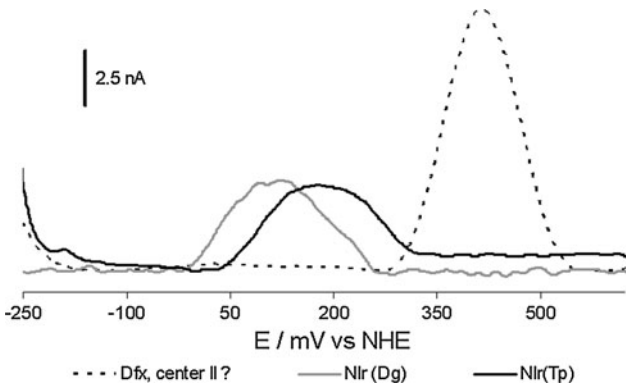

Fig. 7 *Square wave* responses of the Nlr (*Dg*), Nlr (*Tp*) and the more anodic process of Dfx that may be related to center II on gold; 10 mV step potential, 50 mV amplitude and 8 Hz frequency. *Line* smoothing and *baseline* corrections were applied for better visualization

DfxN (overexpression of the C and N-terminal domains, designated by DfxC and DfxN) enabled us to obtain structures containing only one metal center (center II) (Ascenço 2001), which pointed to a midpoint potential of 247 mV. Despite the difference between our results and those of previous reports (Ascenço 2001; Folgosa et al. 2011), we tentatively assigned this process to Dfx center II. Also other authors have found the values of -7 and 430 mV for center I and II, respectively, for another Dfx, purified from *Desulfoarculus baarsii*, which agrees with our results (Berthomieu et al. 2002).

Further studies are necessary to clarify this point; however, we address this process again in the next section for a possible comparison with the Nlr electrochemical response.

Comparison of Dfx with Dx and Nlr

The differences of the direct electrochemical responses of the Dx and Dfx (center I) on the gold electrode can be

Table 2 Formal redox potentials of the metallic centers for the studied proteins obtained by SWV on gold electrodes at room temperature

Protein	$E^{\circ\prime}$/mV versus NHE	
	Center I	Center II
Dx (*Dg*)	+5 ± 7	–
Nl (*Tp*)	–	−97 ± 6
Nl (*Dg*)	–	−30 ± 10
Dfx (*Dv*)	−10 ± 5	+255*

* Folgosa et al. (2011)

clearly seen in Fig. 6. The square wave voltammograms showed, for both proteins, well-defined and reproducible bell-shaped curves. The $E^{\circ\prime}$ values found on gold were −10 and +5 mV versus NHE, respectively, for Dfx and Dx. On GC the formal potential of the two proteins was farther apart (ca. 100 mV), which may be due to the protein's orientation towards the different electrode materials. The Dfx apparently presents better affinity with the modified gold surface than with the carbon electrode. As class II SORs only present one center, similar to Dfx center II, comparison can only be made between the two Nlrs, since the signal from center II of the class I SOR, Dfx, was not clearly assigned. However, there are indications that the additional anodic signal found in Dfx might be related to center II. Despite the need for additional assays, it was decided to add this redox response to the comparison of the results obtained for the Nlr proteins. The SWV of both Nlrs and the redox process, which may be due to Dfx center II, scanned in the anodic direction, are presented in Fig. 7. As can be observed, the Nlrs presented a poor response when the scanning was set in the anodic direction. Both Nlrs present defined redox potentials, ca. 70 mV apart, quite different from the process that might be Dfx related. This may be due to the thermodynamic stability of Dfx center II, which in the ready state presents the iron always reduced in the state Fe(II). The overall Dfx behavior seemed in accordance with the biological relevance of center I, which may have not only a structural function, but also an electron transfer function for center II (Folgosa et al. 2011). In Table 2, a brief summary of the results, using gold electrodes and by SWV, is displayed.

Final remarks

The redox features of the Dfx and its related proteins were observed at GC and gold electrodes by cyclic and SWV techniques. The Dfx presents fewer reversible redox processes and lower peak currents compared with Dx. Although the Nlr (*Dg*) and Nlr (*Tp*) proteins have similar iron centers, their electrochemical features are different. Dfx center I and Dx features are similar, and both present higher formal redox potentials than Nlr, from both class II and III SORs. Dfx center II was not clearly identified, although a more anodic process was observed that may be related to this center.

Acknowledgments Cristina M. Cordas and Patrícia Raleiras wish to acknowledge the Fundação para a Ciência e Tecnologia for the scholarships SFRH/BD/2917/2000 and SFRH/BD/3095/2000, respectively. Requimte is funded by grant PEst-C/EQB/LA0006/2011 from FCT/MCTES.

References

Allen PM, Allen H, Hill O, Walton NJ (1984) Surface modifiers for the promotion of direct electrochemistry of cytochrome *c*. J Electroanal Chem 178(1):69–86

Angove HC et al (2002) Protein film voltammetry reveals distinctive fingerprints of nitrite and hydroxylamine reduction by a cytochrome *c* nitrite reductase. J Biol Chem 277(26):23374–23381

Archer M et al (1995) Crystal structure of desulforedoxin from *Desulfovibrio gigas* determined at 1.8 Å resolution: a novel non-heme iron protein structure. J Mol Biol 251(5):690–702

Armstrong FA, Cox PA, Hill HAO, Lowe VJ, Oliver BN (1987) Metal ions and complexes as modulators of protein-interfacial electron transport at graphite electrodes. J Electroanal Chem 217(2):331–366

Ascenço C (2001) Caracterização Estrutural e Funcional de Proteínas contendo Centros Mononucleares de Ferro Não-Hémico. FCT-UNL, Lisboa

Ascenso C et al (2000) Desulfoferrodoxin: a modular protein. J Biol Inorg Chem 5(6):720–729

Auchère F et al (2004) Overexpression and purification of *Treponema pallidum* rubredoxin: kinetic evidence for a superoxide-mediated electron transfer with the superoxide reductase neelaredoxin. J Biol Inorg Chem 9(7):839–849

Auchère F et al (2006) Kinetics studies of the superoxide-mediated electron transfer reactions between rubredoxin-type proteins and superoxide reductases. J Biol Inorg Chem 11(4):433–444

Berthomieu C et al (2002) Redox-dependent structural changes in the superoxide reductase from *Desulfoarculus baarsii* and *Treponema pallidum*: a FTIR study. Biochemistry 41(32):10360–10368

Bianco PH, Haladjian J (1997) Electrochemistry of ferredoxin and *c*-type cytochromes at surfactant film-modified pyrolytic graphite electrodes. Electrochim Acta 42(4):587–594

Brett AMO, Brett CMA (1996) Electroquímica-Princípios, Métodos e Aplicações. Livraria Almedina, Coimbra

Chattopadhyay KMS (2000) Direct electrochemistry of heme proteins: effect of electrode surface modification by neutral surfactants. Bioelectrochemistry 53(1):17–24

Coelho AV, Matias P, Füllop V, Thompson A, Gonzalez A, Carrondo MA (1997) Desulfoferrodoxin structure determined by MAD phasing and refinement to 1.9 Å resolution reveals a unique combination of a tetrahedral FeS_4 centre with a square pyramidal $FeSN_4$ centre. J Biol Inorg Chem 2:680–689

Correia dos Santos MM, Paes de Sousa PM, Simões Gonçalves ML, Ascenso C, Moura I, Moura JJG (2001) Electrochemical studies of rubredoxin from *Desulfovibrio vulgaris* at modified electrodes. J Electroanal Chem 501(1–2):173–179

Correia dos Santos MM, Paes de Sousa PM, Simões Gonçalves ML, Krippahl L, Moura JJG, Lojou É, Bianco P (2003) Electrochemical

studies on small electron transfer proteins using membrane electrodes. J Electroanal Chem 541:153–162
Czaja C et al (1995) Expression of *Desulfovibrio gigas* desulforedoxin in *Escherichia coli*: purification and characterization of mixed-metal isoforms. J Biol Chem 270(35):20273–20277
Dong S, Jinghong L (1997) Self-assembled monolayers of thiols on gold electrodes for bioelectrochemistry and biosensors. Bioelectrochem Bioenerg 42(1):7–13
Folgosa F et al (2011) New spectroscopic and electrochemical insights on a class I superoxide reductase: evidence for an intramolecular electron-transfer pathway. Biochem J 438:485–494
Hagen WR (1989) Direct electron transfer of redox proteins at the bare glassy carbon electrode. Eur J Biochem 182(3):523–530
Hirst J, Armstrong FA (1998) Fast-scan cyclic voltammetry of protein films on pyrolytic graphite edge electrodes: characteristics of electron exchange. Anal Chem 70(23):5062–5071
Hu N (2001) Direct electrochemistry of redox proteins or enzymes at various film electrodes and their possible applications in monitoring some pollutants. Pure Appl Chem 73(12):1979–1991
Kounaves SP, O'Dea JJ, Chandresekhar P, Osteryoung J (1987) Square wave anodic stripping voltammetry at the mercury film electrode: theoretical treatment. Anal Chem 59(3):386–389
Laviron E (1979) General expression of the linear potential sweep voltammogram in the case of diffusionless electrochemical systems. J Electroanal Chem 101(1):19–28
Laviron E, Roulluier L (1980) General expression of the linear potential sweep voltammogram for a surface redox reaction with interactions between the adsorbed molecules: applications to modified electrodes. J Electroanal Chem 115(1):65–74
Lojou É, Blanco P (2000) Membrane electrodes can modulate the electrochemical response of redox proteins: direct electrochemistry of cytochrome *c*. J Electroanal Chem 485(1):71–80
Lombard M et al (2000) Reaction of the desulfoferrodoxin from *Desulfoarculus baarsii* with superoxide anion: evidence for a superoxide reductase activity. J Biol Chem 275(1):115–121
Lu Z et al (2000) Electroactive films of alternately layered polycations and iron–sulfur protein putidaredoxin on gold. J Colloid Interface Sci 224(1):162–168
Moura I et al (1990) Purification and characterization of desulfoferrodoxin: a novel protein from *Desulfovibrio desulfuricans* (ATCC 27774) and from *Desulfovibrio vulgaris* (strain Hildenborough) that contains a distorted rubredoxin center and a mononuclear ferrous center. J Biol Chem 265(35):21596–21602
Niviere V, Fontecave M (2004) Discovery of superoxide reductase: an historical perspective. J Biol Inorg Chem 9(2):119–123
Osteryoung JG, Rao AO (1885) Square wave voltammetry. Anal Chem 57(1):101–110
Pereira AS et al (2007) Superoxide reductases. Eur J Inorg Chem 2007(18):2569–2581
Razumas VJ, Jasaitis JJ, Kulys JJ (1984) Electrocatalysis on enzyme-modified carbon materials. Bioelectrochem Bioenerg 12(3–4): 297–322
Rusnak F et al (2002) Superoxide reductase activities of neelaredoxin and desulfoferrodoxin metalloproteins. Methods Enzymol 349: 243–258
Souza D, Machado SAS, Avaca LA (2003) Square wave voltammetry. Part I: theoretical aspects. Quim Nova 26(1):81–89
Taniguchi I, Funatsu T, Umekita K, Yamaguchi H, Yasukouchi K (1986) Effect of poly-L-lysine addition on the redox behavior of horse heart cytochrome *c* at functional electrodes. J Electroanal Chem 199(2):455–460
van Os PJHJ, Bult A, Koopal CGJ, van Bennekom WP (1996) Glucose detection at bare and sputtered platinum electrodes coated with polypyrrole and glucose oxidas. Anal Chim Acta 335(3):209–216
Yeh AP et al (2000) Structures of the superoxide reductase from *Pyrococcus furiosus* in the oxidized and reduced states. Biochemistry 39(10):2499–2508
Zhang Z, Rusling JF (1997) Electron transfer between myoglobin and electrodes in thin films of phosphatidylcholines and dihexadecylphosphate. Biophys Chem 63(2–3):133–146